MERIT Self-directed Joint Research

Investigation of quantum criticality of the low-temperature magneto-thermoelectricity in ferromagnet CoMnSb

Hiroto Nakamura[1], Minatsu Koike[2]

[1]Department of Advanced Materials, Graduate School of Frontier Sciences, Univ. of Tokyo

[2]Department of Physics, Graduate School of Science, Gakushuin University

Authors introduction

Hiroto Nakamura: Specializes in single-crystal growth of intermetallic and thermoelectric measurement. In this research, he prepared the single-crystalline sample and analyzed the measurement data.

Minatsu Koike: Specializes in low-temperature physical properties measurement. In this research, she designed and developed the measurement insert for low-temperature Nernst measurement.

Abstract

Anomalous logarithmic temperature dependence of the transverse thermoelectric conductivity, which violates the Mott relation, is expected to appear in the Weyl semimetal state in the vicinity of quantum Lifshitz transition. The temperature range of observing this anomaly indicates the energy scale between the Fermi level and Weyl semimetal state. We developed a new measurement system for the Nernst effect at low temperatures below 30 K, where the conventional measurement system fails to measure it, and achieved lower uncertainty. The Nernst coefficient and transverse thermoelectric conductivity quantitatively match the previous work within the error bar. The energy scale estimated from the saturating temperature of the logarithmic temperature dependence of the transverse thermoelectric conductivity is consistent with the sample's Fermi level and predicted Weyl semimetal state.

1. Research Background and Motivation

Topological band structures in materials are widely known to generate large Berry curvature. Berry curvature behaves as a fictitious magnetic field to carriers and causes anomalous Hall effect (AHE) and anomalous Nernst effect (ANE) perpendicular to electric current or thermal gradient. Therefore, huge AHE or ANE can be one of the strong indicators of the topological band structure in materials. Notable AHE and ANE are observed in small magnetization magnet Mn_3Sn [1] and $YbMnBi_2$ [2], and ferromagnet Co_2MnGa [3] and $Co_3Sn_2S_2$ [4], which are considered to originate from one of the topological states, namely Weyl semimetal state.

The transverse thermoelectric conductivity α_{yx}, usually dominating large ANE of topological

band structure, is the transport coefficient sensitive to the density of states and Berry curvature around the Fermi energy E_F. In ferromagnet Co$_2$MnGa, a less-dispersed energy band composing Weyl semimetal state is predicted by first-principles calculation and it is tuned just around the Lifshitz transition, namely a dramatic change of the topology of the Fermi surface. The scaling behavior of transported coefficient around this quantum phase transition is proposed in the theoretical model and observed in the experiment [3].

In this situation, if $|E_F - E_0| \approx 0$ is achieved, where E_0 represents the energy of Weyl point (the crossing point of linear dispersion in Weyl semimetal state), the behavior of $\alpha_{yx}/T \sim \ln T$ is predicted down to the lowest temperature, violating the behavior $\alpha_{yx}/T \sim$ const. derived from Mott relation. Even when E_F is not close to the Weyl point, the same behavior is predicted and observed above the temperature corresponding to $|E_F - E_0|$ of energy scale (Fig. 1).

Fig. 1: Temperature dependence of the transverse thermoelectric conductivity α_{yx} in Co$_2$MnGa [3]. The dashed line shows the model calculation at $|E_F - E_0| \approx 0$. The model calculation at slightly shifted E_F (dark solid line) describes well the experiment values (red mark) and the first-principles calculation (blue mark).

Recently, we observed similar behavior in ferromagnet CoMnSb and $\alpha_{yx}/T \sim \ln T$ seems to be observed down to low temperature. Hence, the sample's Fermi energy is indicated to be tuned close to the Weyl point [5].

However, the Nernst coefficient is usually in the order of 0.1 µV/K or smaller and the thermal gradient will be also limited to achieving linear response at low temperature, so the signal size of ANE can be less than 100 nV. The ANE signal measured in the Thermal Transport Option (TTO) of the Physical Property Measurement System (PPMS) by Quantum Design Inc., widely used for thermoelectric measurement below room temperature, is hindered by noise and produces large uncertainty below 30 K. Because the off-diagonal component of the product of electric conductivity and thermoelectric coefficients tensors, namely α_{yx}, also has a large uncertainty, the temperature range of observing $\alpha_{yx}/T \sim \ln T$ was ambiguous. Here, we developed a new measurement insert while utilizing the temperature controller and superconducting magnet of the PPMS to perform a high-quality measurement of the Nernst coefficient.

2. Experimental Method

Sample preparation

The single-crystalline sample of CoMnSb grown by Prof. Nugroho (ITB) using the Czochralski

method was cut into a rectangular bar by spark erosion. The magnetic field direction and thermal gradient direction are set to $[0\ 1\ 1]$ and $[2\ \bar{1}\ 1]$, respectively. The crystal orientation was determined by the back-scattering Laue method (Fig. 2). To apply the 1D thermal gradient along $[2\ \bar{1}\ 1]$, the length along the thermal gradient was made longer and the thickness along the magnetic field was made thinner. After polishing the sample's surface to minimize radiation, the 15 μm diameter gold wires to thermally contact the thermal bath, thermometer, and heater and to measure the Nernst thermoelectricity were added.
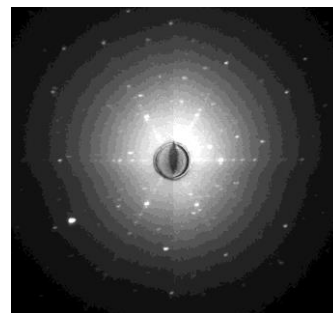
Fig. 2: Laue diffraction image of $(1\ 1\ \bar{1})$ in CoMnSb single crystal. The horizontal and vertical directions are $[2\ \bar{1}\ 1]$ and $[0\ 1\ 1]$, respectively.

Thermal transport measurement

Figure 3 shows the schematic figure of the measurement cell around the sample. One side of the sample is connected to the copper block thermal bath using silver paste (DuPont 4922N). The Joule heat generated by the heater was conducted through the gold wire and the sample and the thermal gradient and Nernst thermoelectric response were measured in the steady-state. The thermal conductivity was obtained from the thermal gradient and heater power, and the Nernst coefficient was obtained from the thermal gradient and the voltage perpendicular to the magnetic field and heat current. The Cernox resistivity thermometer was used to measure the temperature of the sample and connected to the sample through gold wires as well. In addition, a long spring of low thermally conductive metal was adopted for the electric wires of the heater and thermometers to avoid heat exchange other than the sample. The sample chamber was in a high vacuum to avoid convection
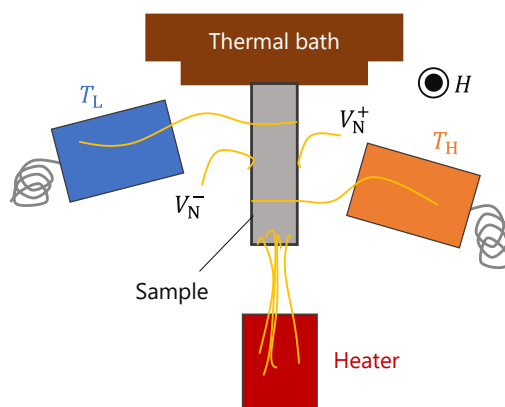
Fig. 3: The measurement setting of thermal transport measurement cell. The resistance heater and thermometers are thermally connected through gold wire to the sample. The magnetic field H is applied out of plane.

heat transfer. For the high-quality measurement of the Nernst voltage below 100 nV, we used the 2182A Nanovoltmeter (Keithley).

3. Result and Discussion

Before the Nernst effect measurement, we estimated the heater power enough to observe the signal. The temperature difference between the two thermometers was applied in the ratio of 0.5%, 1%, 2%, and 10% to the thermal bath temperature. Figure 4(a) shows the temperature dependence of the thermal conductivity observed in this measurement. The thermal conductivity measured by the PPMS thermal transport option (TTO) is also shown in the same figure as a reference. First, the values of the thermal conductivity do not have any dependence on temperature difference, so Fourier's law is confirmed in any temperature differences. Therefore, even at the temperature difference of 10%, uniform and linear thermal gradient along the $[2\,\bar{1}\,1]$ direction was verified. Second, the thermal conductivity in this measurement deviates from those measured in PPMS-TTO above 30 K. Even in a high vacuum condition, heat loss from the heater and thermometers can happen because of radiation or heat conduction via electric wire. In this condition, two scenarios can be considered: (i) overestimating the heat flow from the heater to the sample and (ii) the temperature difference between two thermometers deviates from the actual temperature difference in the sample. Scenario (i) only affects the estimation of thermal conductivity, but (ii) does both the thermal conductivity and Nernst coefficient. As shown in Fig. 4(b), the values of the Nernst coefficient also deviate in a similar temperature range, so at least scenario (ii) seems to influence our measurement. We mainly aim at high-quality Nernst effect measurement at the low temperature, so the measurement results below 30 K will be discussed from here on.
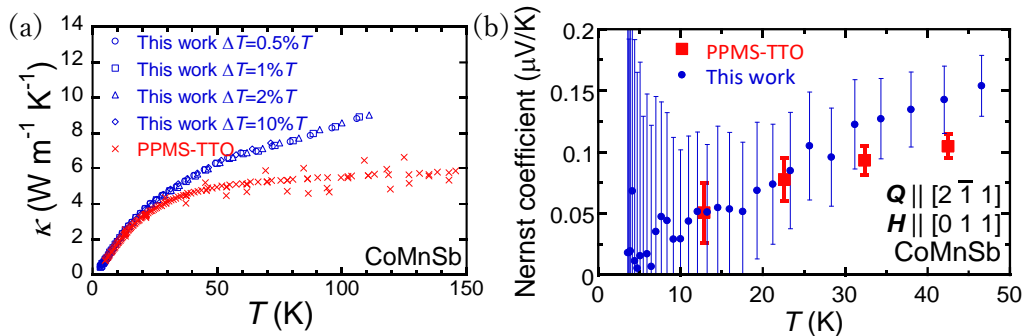
Fig. 4: (a) The temperature dependence of the thermal conductivity. The blue marks show the result of this work with four patterns of the temperature difference (see main text). The red marks show the result measured by the PPMS thermal transport option (TTO). (b) The temperature dependence of the Nernst coefficient calculated from the thermoelectric signal measured at the same time as the thermal conductivity.
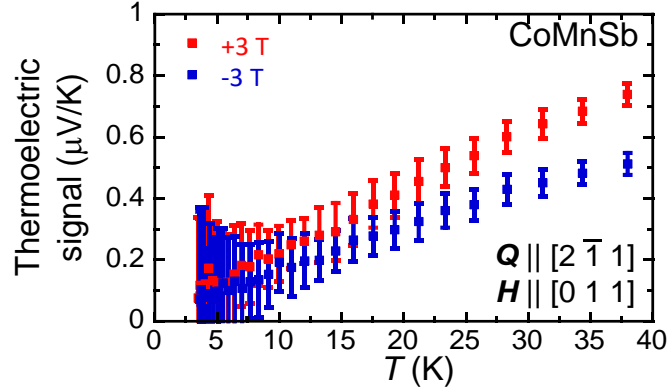
Fig. 5: The temperature dependence of the thermoelectromotive force caused by Nernst effect at the magnetic field of +3 T and -3 T.

In the Nernst coefficient measurement, the temperature difference of 10% to the thermal bath temperature was applied and the temperature sweep was performed in the magnetic field of +3 T and -3 T. Because the thermoelectric signal of the Nernst effect is antisymmetric to the magnetic field, the Nernst coefficient can be obtained by taking the difference of the thermoelectromotive force between +3 T and -3 T. However, as shown in Fig. 5, the large error bar overlapping below 20 K makes it difficult to estimate the Nernst coefficient correctly. In our measurement, the thermoelectric voltage was measured as 90 times average with or without thermal gradient at each temperature. The error bar represents the statistical error of each measurement. The thermoelectric voltage without thermal gradient was measured for the background voltage other than the thermoelectric effect. We consider the error of the Nernst coefficient to become large because taking the difference from the background and among positive/negative fields causes underflow.

Figure 6 shows the magnetic field dependence of the Nernst coefficient measured when the sample middle temperature is 6.3 K, 12 K, and 24 K. Except for the result at 6.3 K with a large error
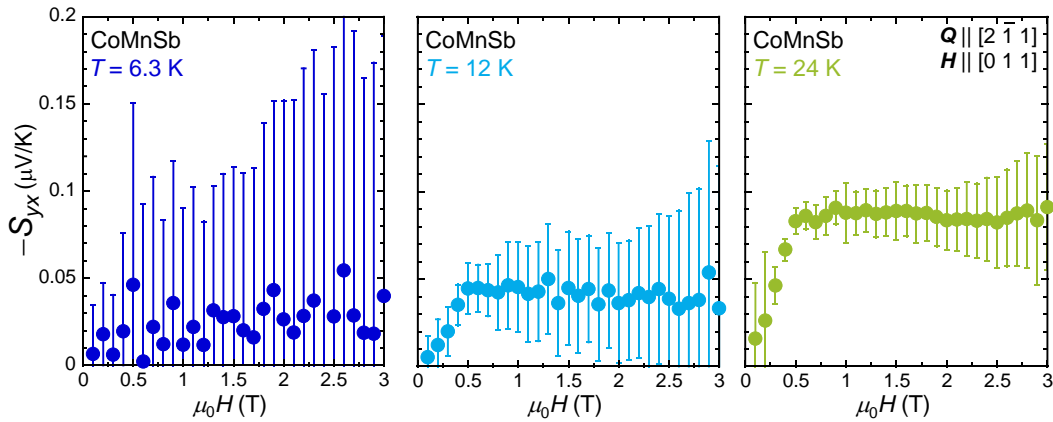
Fig. 6: The magnetic field dependence of the Nernst coefficient. The measurements were performed when the sample middle temperature is 6.3 K, 12 K, and 24 K respectively.
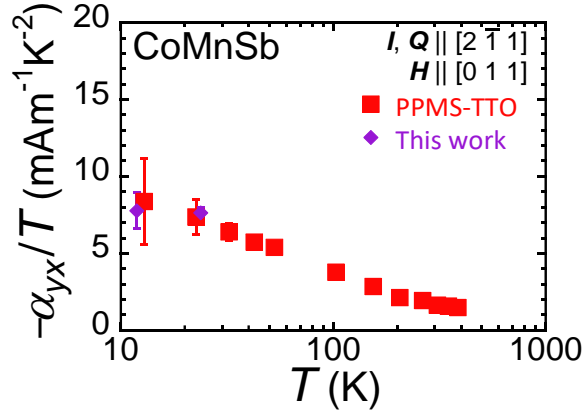
Fig. 7: The temperature dependence of the transverse thermoelectric conductivity divided by temperature α_{yx}/T. The values calculated from the Nernst coefficient at 12 K and 24 K in our measurement (purple marks), and from those measured by PPMS-TTO (red marks) are shown with error bars.

compared to the measured value, the typical behavior of ANE saturating around the magnetic field of 0.5 T was observed. The larger error at the higher magnetic field indicates some magnetic noise included in the signal, so the improvement of electric wire connection or shielding would be necessary. Here, we define the Nernst coefficient at each temperature as the average at 1–2 T, where the values saturate and the error is relatively small.

Finally, we calculated the transverse thermoelectric conductivity $\alpha_{yx} = \sigma_{yy}S_{yx} + \sigma_{yx}S_{xx}$, where S_{yx} is the Nernst coefficient we measured in this work, the longitudinal electrical conductivity σ_{yy}, the Hall conductivity σ_{yx}, and the Seebeck coefficient S_{xx} measured by PPMS using the sample in the same batch. Figure 7 shows the semi-log plot of the temperature dependence of the transverse thermoelectric conductivity divided by the temperature α_{yx}/T. The α_{yx}/T values calculated using our measurement result around 12 K and 24 K match well within the error bar with those using the PPMS-TTO result, while the size of the error becomes much smaller, indicating we could successfully perform higher quality and accurate measurement using our home-made measurement insert. We observe $\alpha_{yx}/T \sim \ln T$ behavior down to 24 K but the saturation seems to occur around 12 K. If the saturation temperature of $\alpha_{yx}/T \sim \ln T$ is estimated as approximately 20 K, the corresponding energy scale is 1.7 meV. Indeed, the Weyl semimetal state with its Weyl point at $E_F = -132$ meV was predicted by first-principles calculation, which is close to -130 meV estimated experimentally from the sample composition and the comparison of transport coefficients with the calculation [5]. In conclusion, if this Weyl semimetal state is in the vicinity of the Lifshitz transition, our observation of $\alpha_{yx}/T \sim \ln T$ above 24 K is consistent with the theoretical prediction.

4. Conclusion and Future Prospect

In this work, we developed the measurement system to measure the thermoelectric effect accurately at low temperatures and observed the anomalous Nernst effect in ferromagnet CoMnSb. The Nernst effect below 30 K obtained from the magnetic field dependence of the thermoelectromotive force matched quantitatively with the previous measurement in the commercial system, and its error was suppressed a lot. By removing the heat loss and the noise at a high magnetic field, more accurate measurement in a wider temperature range is expected. The energy scale where the Weyl semimetal state around the Lifshitz transition influences the transport coefficients was calculated from the logarithmic temperature dependence of the transverse thermoelectric conductivity divided by the temperature. As a result, we obtained consistent results compared to the distance between the sample's Fermi level and the Weyl point estimated in the previous work.

References

[1] M. Ikhlas and T. Tomita *et al.*, *Nat. Phys.* 13, 1085 (2017).

[2] Y. Pan *et al.*, *Nat. Mater.* 21, 203 (2021).

[3] A. Sakai *et al.*, *Nat. Phys.* 14, 1119 (2018).

[4] S. N. Guin *et al.*, *Adv. Mater.* 31, 1806622 (2019).

[5] H. Nakamura *et al.*, *Phys. Rev. B* 104, L161114 (2021).